RIM1α phosphorylation at serine-413 by protein kinase A is not required for presynaptic long-term plasticity or learning

Pascal S. Kaeser*[†], Hyung-Bae Kwon[‡], Jacqueline Blundell[§], Vivien Chevaleyre[‡¶], Wade Morishita[‖], Robert C. Malenka[‖], Craig M. Powell[§**], Pablo E. Castillo[‡], and Thomas C. Südhof*[†,††‡‡§§]

Departments of *Neuroscience, [§]Neurology, [††]Molecular Genetics, and **Psychiatry and [‡‡]Howard Hughes Medical Institute, University of Texas Southwestern Medical Center, Dallas, TX 75390; [‡]Dominick P. Purpura Department of Neuroscience, Albert Einstein College of Medicine, Bronx, NY 10461; and [‖]Department of Psychiatry and Behavioral Sciences, Nancy Pritzker Laboratory, Stanford University School of Medicine, Palo Alto, CA 94304

Contributed by Thomas C. Südhof, July 11, 2008 (sent for review June 6, 2008)

Activation of presynaptic cAMP-dependent protein kinase A (PKA) triggers presynaptic long-term plasticity in synapses such as cerebellar parallel fiber and hippocampal mossy fiber synapses. RIM1α, a large multidomain protein that forms a scaffold at the presynaptic active zone, is essential for presynaptic long-term plasticity in these synapses and is phosphorylated by PKA at serine-413. Previous studies suggested that phosphorylation of RIM1α at serine-413 is required for presynaptic long-term potentiation in parallel fiber synapses formed *in vitro* by cultured cerebellar neurons and that this type of presynaptic long-term potentiation is mediated by binding of 14-3-3 proteins to phosphorylated serine-413. To test the role of serine-413 phosphorylation *in vivo*, we have now produced knockin mice in which serine-413 is mutated to alanine. Surprisingly, we find that in these mutant mice, three different forms of presynaptic PKA-dependent long-term plasticity are normal. Furthermore, we observed that in contrast to RIM1α KO mice, RIM1 knockin mice containing the serine-413 substitution exhibit normal learning capabilities. The lack of an effect of the serine-413 mutation of RIM1α is not due to compensation by RIM2α because mice carrying both the serine-413 substitution and a RIM2α deletion still exhibited normal long-term presynaptic plasticity. Thus, phosphorylation of serine-413 of RIM1α is not essential for PKA-dependent long-term presynaptic plasticity *in vivo*, suggesting that PKA operates by a different mechanism despite the dependence of long-term presynaptic plasticity on RIM1α.

active zone | neurotransmitter release | Rab3 | synaptic vesicle | mossy fiber

Synaptic long-term potentiation (LTP) and long-term depression (LTD) are central processes in the nervous system that mediate use-dependent changes in synaptic transmission and are implicated in many forms of learning and memory (1). Different subsets of synapses exhibit distinct forms of long-term plasticity. The more widely studied postsynaptic form of LTP is induced by an NMDA receptor-dependent mechanism and involves the regulation of AMPA-type glutamate receptors (2, 3). However, excitatory synapses, such as those formed by hippocampal mossy fibers (4, 5), cerebellar parallel fibers (6, 7), and the corticostriatal (8) and corticothalamic connections (9), as well as inhibitory synapses that contain presynaptic cannabinoid receptors (10, 11), express presynaptic forms of long-term plasticity. A common feature of these types of plasticity is that induction of long-term plasticity depends on protein kinase A (PKA) activation, and expression is due to changes in the amount of neurotransmitter release evoked by an action potential (12, 13). In these synapses, calcium entry triggers the calcium/calmodulin-sensitive adenylyl cyclase to synthesize cAMP, which in turn activates presynaptic PKA. PKA activation is required for presynaptic long-term plasticity (reviewed in ref. 14).

Two presynaptic proteins seem to be essential for most if not all forms of PKA-dependent long-term plasticity: the low-molecular-weight GTP-binding protein Rab3A, which is localized to synaptic vesicles, and its effector protein RIM1α, which is localized to active zones (15, 16). In contrast, other proteins, such as synapsins and rabphilins—both of which are PKA substrates—are not required for presynaptic, PKA-dependent, long-term plasticity (17, 18). These findings indicated that a presynaptic pathway that involves binding of Rab3A on synaptic vesicles to RIM1α in the presynaptic active zone mediates presynaptic plasticity but did not reveal how PKA regulates their function in presynaptic long-term plasticity. The discovery that RIM1α is a substrate for PKA at two sites (serine-413 and serine-1548), and that in cultured cerebellar neurons, serine-413 but not serine-1548 was essential for long-term presynaptic plasticity, raised the possibility that PKA acts by phosphorylating serine-413 (19). Consistent with this notion, phosphorylation of serine-413 in RIM1α was shown to induce binding of 14-3-3 proteins, and this binding was found to regulate neurotransmitter release (20).

Because of the central importance of presynaptic long-term plasticity in brain function, we have now tested the relevance of serine-413 phosphorylation of RIM1α, and 14-3-3 binding to RIM1α *in vivo*. We show that phosphorylated serine-413 is the only tight binding site for 14-3-3 proteins in RIM1α and that 14-3-3 binding is dependent on phosphorylation of serine-413. More importantly, we show that in mice, mutating serine-413 to alanine abolishes RIM1α phosphorylation and 14-3-3 protein binding *in vitro* but does not detectably alter presynaptic long-term plasticity. Our data thus suggest that, although the Rab3A/RIM1α complex is essential for presynaptic long-term plasticity, PKA regulates this type of plasticity by a mechanism that is distinct from its phosphorylation of RIM1α.

Results

Phosphoserine-413 Represents the Only Tight 14-3-3 Binding Site in RIM1α. To identify specific interaction partners for RIM1α phosphorylated on serine-413, we performed affinity chromatography experiments with phosphorylated GST-fusion proteins.

Author contributions: P.S.K., R.C.M., C.M.P., P.E.C., and T.C.S. designed research; P.S.K., H.-B.K., J.B., V.C., W.M., and C.M.P. performed research; P.S.K. contributed new reagents/analytic tools; P.S.K., H.-B.K., J.B., V.C., W.M., R.C.M., C.M.P., P.E.C., and T.C.S. analyzed data; and P.S.K., R.C.M., C.M.P., P.E.C., and T.C.S. wrote the paper.

The authors declare no conflict of interest.

[†]Present address: Department of Molecular and Cellular Physiology and Neuroscience Institute, Stanford University School of Medicine, Palo Alto, CA 94304-5543.

[¶]Present address: Department of Neuroscience, Columbia University, New York, NY 10032.

[§§]To whom correspondence should be sent at the present address: Department of Molecular and Cellular Physiology and Neuroscience Institute, Stanford University School of Medicine, Palo Alto, CA 94304-5543. E-mail: tcs1@stanford.edu.

This article contains supporting information online at www.pnas.org/cgi/content/full/0806679105/DCSupplemental.

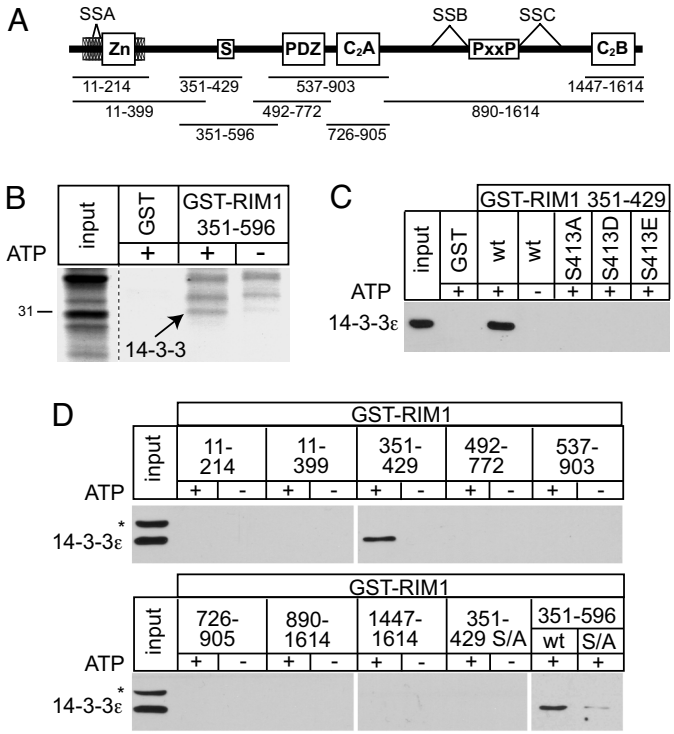

Fig. 1. RIM1α contains a single tight 14-3-3 binding site. (*A*) Schematic overview of RIM1α and its protein domains. GST-fusion proteins that were used for the biochemical characterization are indicated. SSA, SSB, SSC, splice site A, B, and C; PxxP, proline-rich sequence; S, serine-413 phosphorylation site. (*B*) Coomassie blue staining of the eluates of the affinity column that contained phosphorylated GST-RIM1 351–596 and nonphosphorylated control RIM1α. The arrow indicates the phospho-specific band that was submitted to mass spectrometry. (*C*) *In vitro* binding of wild-type (wt) and mutant GST-RIM1 351–429 to 14-3-3ε in GST-pulldown experiments from rat brain homogenates. (*D*) *In vitro* binding of PKA phosphorylated and nonphosphorylated GST-RIM1 fusion proteins to 14-3-3ε in GST pulldown experiments from brain homogenates. S/A, S413A-point mutant RIM1α fragment; wt, wild-type RIM1 fragment; *, cross-reactive band that sometimes appears in fresh brain homogenates with the 14-3-3ε antibody.

We purified RIM1-GST fusion proteins containing residues 351–596 of RIM1α, incubated them with PKA in the presence or absence of ATP, and coupled them to amino-link chromatography columns. We then bound solubilized rat brain proteins containing phosphatase inhibitors to the column and analyzed bound proteins by SDS/PAGE and Coomassie staining (Fig. 1 *A* and *B*). One band of $\approx$30 kDa specifically bound to phosphorylated but not to nonphosphorylated RIM1-GST fusion protein and was analyzed by mass spectroscopy and immunoblotting. We found that this band consisted of multiple isoforms of 14-3-3 proteins (14-3-3ε, 14-3-3η, and 14-3-3ζ; Fig. 1*B*). We confirmed this finding with GST-pulldown experiments using GST-RIM1α fusion proteins that contain residues 351–429 and 351–596 of RIM1α [supporting information (SI) Fig. S1], and our data are consistent with previously reported binding of phosphorylated RIM1α to 14-3-3 proteins (20).

To test whether the affinity chromatography results reflect a specific binding reaction and whether other sequences of RIM1α also bind to 14-3-3 proteins, we performed additional GST-pulldown experiments using phosphorylated and nonphosphorylated GST-RIM1α fusion proteins. We first examined 14-3-3 binding to GST-fusion proteins containing residues 351–429 of RIM1α, either with a wild-type sequence or with mutations that substitute serine-413 for alanine, aspartate, or glutamate. These mutations were used to test not only the phosphorylation dependence of 14-3-3 protein binding with the alanine substitution, but also the specificity of 14-3-3 protein binding with the aspartate and glutamate substitutions that are thought to mimic phosphorylated serines and threonines for some phosphoserine and -threonine residues (21) but are known to be inactive for 14-3-3 proteins (22). Indeed, we found that all three substitutions (serine to alanine, serine to aspartate, and serine to glutamate) inactivated binding of 14-3-3 proteins to RIM1α (Fig. 1*C*).

We next tested whether RIM1α contains other tight binding sites for 14-3-3 proteins. This test was prompted by the fact that 14-3-3 proteins usually occur as dimers and function to induce conformational changes, to mask protein domains, or to scaffold proteins (23), and was further motivated by a previous study indicating that RIM1α binds 14-3-3 proteins in a phosphorylation-independent manner between residues 241 and 287 (24). For this purpose, we used GST-fusion proteins covering the entire RIM1α sequence (Fig. 1*A*). However, we observed no other 14-3-3 binding sites in RIM1α using GST-pulldown experiments with or without phosphorylation by PKA (Fig. 1*D*). Thus, RIM1α likely contains a single tight binding site for 14-3-3 that is generated by PKA phosphorylation of serine-413, although the presence of additional low-affinity binding sites cannot be excluded.

Generation and Characterization of Knockin Mice Containing a Serine-413 to Alanine Substitution in RIM1α. To test the physiological role of the phosphorylation of RIM1α at serine-413, we used homologous recombination to generate knockin (KI) mice in which the RIM1 gene contains a serine-413 to alanine (S413A) substitution (Fig. 2*A*). In addition to the S413A point mutation, silent BglI and SphI restriction sites were introduced into the ORF for genotyping the S413A mutant locus. Homologous recombination experiments were performed in embryonic stem cells using selection with a neomycin resistance cassette (Fig. 2*A*) and were confirmed in the stem cells and in the mice we generated from them by Southern blotting, PCR, and DNA sequencing (Fig. 2 *B–D*). The neomycin resistance cassette was removed from the mice by flp recombination, resulting in a mouse line that contained only the serine-413 point mutation in exon 6, a single frt recombination site in intron 6, and loxP sites flanking exon 6. This mouse line (referred to as RIM1 S413A-KI mice) was used for all experiments.

RIM1 S413A-KI mice were viable and fertile and exhibited no impairment of survival or loss of weight when compared with littermate wild-type control mice (Fig. 3 *A* and *B*). Immunoblotting showed that RIM1α expression was similar in littermate wild-type and RIM1 S413A-KI mice (Fig. 3*C*). Importantly, a previously characterized phospho-specific antibody directed against phosphorylated serine-413 confirmed a complete absence of phosphoserine-413 RIM1α in RIM1 S413A-KI mice (arrow, Fig. 3*C*). There was a cross-reactive band (marked with and asterisk in Fig. 3*C*) at a slightly lower molecular weight that was present in both the KI and the wild-type control mice. This cross-reactive band is not RIM1α or RIM2α because it is still present in RIM1α or RIM2α KO mice (data not shown). Immunoblotting analyses of other brain proteins failed to detect any major changes in the RIM1 S413A-KI mice (Fig. 3*D*).

Normal Presynaptic Long-Term Plasticity in RIM1 S413A-KI Mice. We next tested whether the mutational block of RIM1α phosphorylation in RIM1 S413A-KI mice impairs presynaptic long-term plasticity using electrophysiological recordings in acute slices from littermate wild-type control and RIM1 S413A-KI mice. Surprisingly, no significant impairment in any form of presynaptic plasticity was detected (Fig. 4 and Table S1). Specifically, measurements of LTP at the cerebellar granule cell to Purkinje cell synapse after repetitive stimulation of parallel fibers failed to detect a decrease in LTP in the RIM1 S413A-KI mice (Fig.

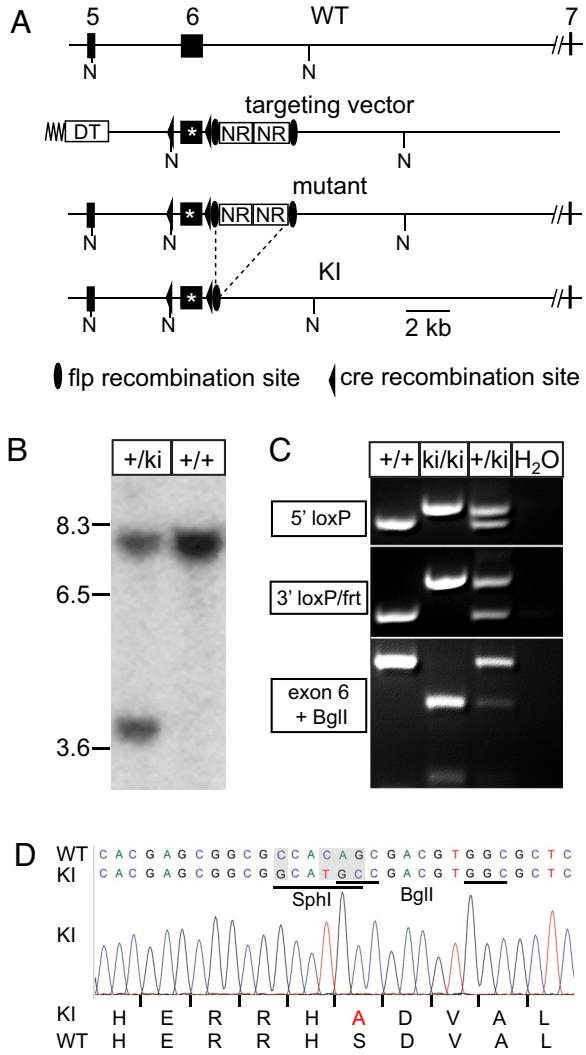

Fig. 2. Generation of RIM1 S413A-KI mice. (*A*) KI strategy for the RIM1 S413A-KI mice showing (from top to bottom) the wild-type (WT) RIM1 allele, the S413A KI targeting construct, the RIM1 mutant allele after homologous recombination, and the flp-excised KI allele. 5, 6, and 7, exons 5, 6 and 7; DT, diphtherotoxin-expressing cassette; NR, neomycin resistance cassette; *, S413A point mutation in exon 6; N, NcoI restriction sites that were used for Southern blotting. (*B*) Southern blot from heterozygous embryonic stem cells after homologous recombination and wild-type control cells, NcoI digest, and a 5′ outside probe were used. The wild-type band is 8.0 kilobases (kb), the KI band 3.8 kb. (*C*) PCR genotyping of the RIM1 S413A-KI mice including heterozygous and wild-type controls for (from top to bottom) the 5′ loxP site, the 3′ loxP/frt site after flp-recombination, and the S413A point mutation/BglI restriction site after BglI digest of the amplified fragments. (*D*) Sequencing result of the homozygous KI allele in RIM1 S413A-KI mice. Wild-type (WT) DNA and protein sequences are indicated for comparison.

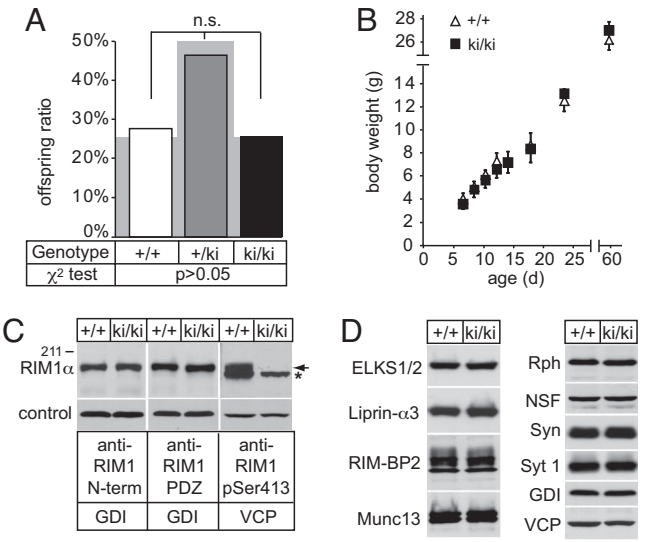

Fig. 3. Basic characterization of the RIM1 S413A-KI mice. (*A*) Survival ratio of offsprings from heterozygous matings of RIM1 S413A-KI mice; the gray shaded area indicates the expected Mendelian ratio. (*B*) Body weight of RIM1 S413A-KI and control littermate mice from postnatal day 6 to 60. (*C*) Western blotting for RIM1α with antibodies against the N terminus (Q703), the central part including the PDZ domain (R809), the phosphoserine-413 residue (T2798; arrow, absence of serine-413-phosphorylated RIM1α; star, cross-reactive band at a slightly lower molecular weight), and loading controls. GDI, GDP dissociation inhibitor; VCP, valosin-containing protein). (*D*) Western blotting of brain homogenates for several presynaptic and other proteins appears normal. Rph, rabphilin; RIM-BP2, RIM-binding protein 2; NSF, *N*-ethylmaleimide-sensitive factor; Syn, synapsin; Syt 1, synaptotagmin-1.

4*A*). Similarly, LTP in hippocampal mossy fiber synapses was unchanged (Fig. 4*B*), as was endocannabinoid-dependent LTD at inhibitory synapses in the CA1 area of the hippocampus (I-LTD; Fig. 4*C*). Thus, different from rescue experiments in cultured neurons (19), presynaptic long-term plasticity in acute brain slices does not require phosphorylation of serine-413 in RIM1α, even though it does require RIM1α itself (11, 16).

The lack of a plasticity phenotype in the RIM1 S413A-KI mice raises the possibility that compensation may have developed with this germline mutation. Although unlikely given that the RIM1α KO also represents a germline mutation and does produce a defect in plasticity (11, 16), we tested this possibility by analyzing mice that carry both the RIM1 S413A-KI mutation and a deletion of RIM2α (25). RIM2α is the only other RIM isoform other than RIM1α that binds to Rab3; thus, any compensation would likely have to operate through this isoform. However, we found that mossy fiber LTP in these double-mutant mice was also unchanged (Fig. 4*D*). Furthermore, parallel fiber LTP was expressed in these double-mutant mice (double-mutant RIM1 S413A-KI/RIM2α KO mice: 138 ± 8%, 5 slices/3 mice; data not shown). These experiments exclude the possibility that RIM2α compensates for the loss of the serine-413 phosphorylation site in RIM1 S413A-KI mice.

In addition to impaired presynaptic long-term plasticity, RIM1α KO mice exhibit a major defect in short-term plasticity at Schaffer collateral to CA1 pyramidal cell synapses (26). We thus also measured two forms of short-term plasticity at these synapses in RIM1 S413A-KI mice, but again we found no difference (Fig. 5 and Table S1). Paired-pulse ratios in response to 2 stimuli applied with a 40-ms interval were unchanged (Fig. 5*A*), as were responses to a train of 25 stimuli at 14 Hz (Fig. 5*B*).

RIM1 S413A-KI Mice Exhibit Normal Behaviors. As a further test of the effect of the RIM1 S413A-KI mutation on brain function, we monitored fundamental behavioral parameters in the RIM1 S413A-KI mice. Behavior is a sensitive test for overall brain function, and RIM1α KO mice exhibit major impairments in multiple behavioral parameters (27).

Using age-matched male littermate pairs that were either wild-type or homozygous mutant for the S413A KI, we found no significant behavioral differences (Fig. 6). Specifically, total activity in a novel mouse cage (mixed ANOVA, $P > 0.4$) was similar in S413A KI and wild-type littermate control mice (Fig. 6*A*; see *SI Materials* and Fig. S2 for the analysis of locomotor habituation and total distance traveled in an open field). Anxiety-like behavior (Fig. 6*B*) as measured by latency to enter the

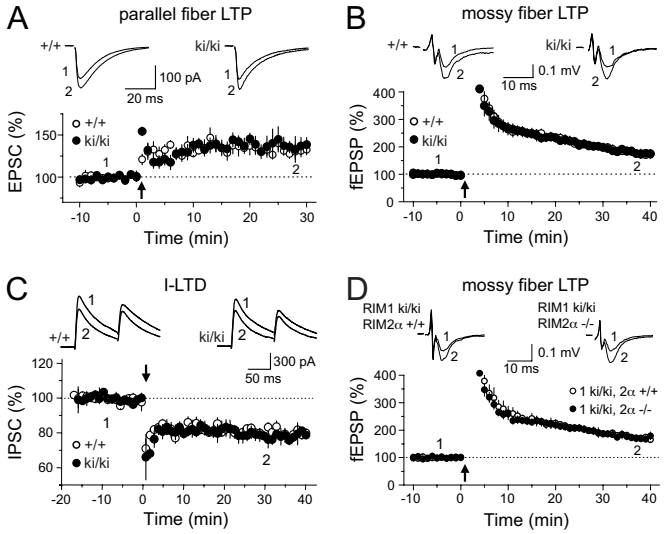

Fig. 4. Cerebellar parallel fiber LTP, mossy fiber LTP, and I-LTD in the hippocampus are normal in RIM1 S413A-KI mice. (*A*) LTP at parallel fiber to Purkinje cell synapses in response to a single tetanus (200 stimuli at 10 Hz, vertical arrow). EPSC, excitatory postsynaptic current. (*B*) LTP at mossy fiber to CA3 pyramidal cell synapses evoked by a tetanus (125 pulses at 25 Hz) delivered to mossy fibers (vertical arrow). A few data points right after tetanization were removed for clarity. fEPSP, field excitatory postsynaptic potential. (*C*) Endocannabinoid-mediated long-term depression at hippocampal inhibitory synapses (I-LTD) in wild-type and mutant mice was induced by theta-burst stimulation (vertical arrow) consisting of a series of 10 bursts of 5 stimuli (100-Hz burst, 200-ms interburst interval), which was repeated 4 times (5 s apart). IPSC, inhibitory postsynaptic current. (*D*) Mossy fiber LTP in RIM1 S413A-KI/RIM2α KO double-mutant and RIM1 S413A-KI control mice. In *A–D*, averaged sample traces taken at times indicated by numbers are shown above summary graphs.

light side of a dark/light box ($P > 0.5$), time spent in the open arms of an elevated plus maze ($P > 0.7$), time spent in the center of an open field ($P > 0.7$), and motor coordination (Fig. 6*C*) were also unchanged in the RIM1 S413A-KI mice. Two forms of learning and memory that were severely affected in the RIM1α KO mice showed no impairment in the RIM1 S413A-KI mice. Twenty-four hours after training in context- and cue-dependent fear conditioning, both wild-type and RIM1 S413A-KI mice

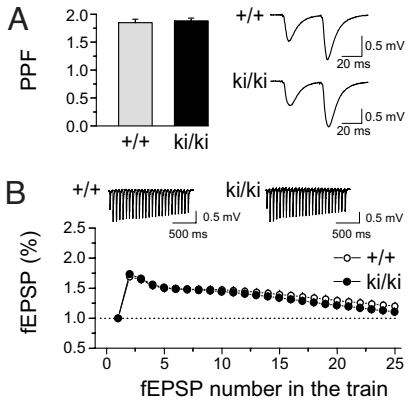

Fig. 5. Short-term synaptic plasticity in RIM1 S413A-KI mice in excitatory Schaffer collateral to CA1 pyramidal neuron synapses. (*A*) Summary graph (*left*) and averaged sample traces (*right*) of paired pulse facilitation (PPF) measured at 40-ms interstimulus interval in RIM1 S413A-KI and control mice. (*B*) Synaptic responses [field excitatory postsynaptic potentials (fEPSPs)] elicited by a 14-Hz train of 25 stimuli in RIM1 S413A-KI and control mice. Values are normalized to the first synaptic response of the stimulation train.

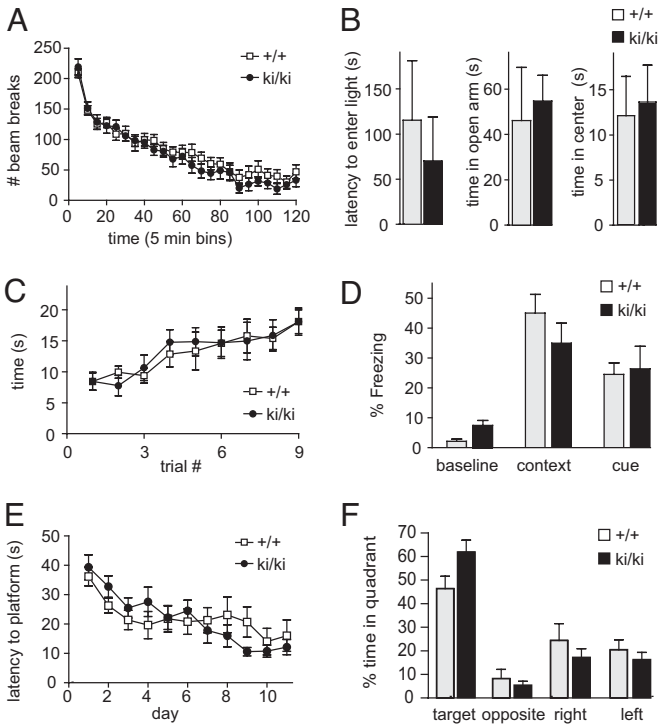

Fig. 6. RIM1 S413A-KI mice displayed normal locomotor activity, anxiety-like behavior, motor coordination, and spatial and emotional learning and memory. (*A*) Measurements of the spontaneous motor activity of RIM1 S413A-KI and control mice were determined as the number of beam breaks per minute in a fresh home cage equipped with photodetector beams. (*B*) Anxiety-related behaviors probed as latency to enter the light side of a dark/light box, as the time spent in the open arms of an elevated plus maze, and as the time spent in the center of an open field. (*C*) Measurements of motor coordination monitored as the time mice stay on an accelerating rotarod as a function of trial number. (*D*) Freezing behavior to both context- and cue-dependent fear conditioning 24 h after training. (*E*) Morris water maze analysis of spatial learning during the initial 11 days of training as measured by latency to reach the submerged platform. (*F*) Spatial memory test on day 12 of the Morris water maze analysis after removal of the platform from the target quadrant. Percent time spent in each quadrant is indicated.

displayed similar cue ($P > 0.8$) and contextual ($P > 0.2$) fear conditioning (Fig. 6*D*). During training in the Morris water maze, latency to reach a submerged platform was similar in RIM1 S413A-KI mice (Fig. 6*E*; mixed ANOVA, $P > 0.3$) and the control mice. Furthermore, RIM1 S413A-KI and control mice displayed a significant preference for the target vs. all other quadrants on day 12 after removal of the platform in the probe trial (Fig. 6*F*; wildtype and RIM1 S413A-KI = $P < 0.05$). Distance traveled, swim speed, and thigmotaxis were also normal in the RIM1 S413A-KI mice (data not shown). Taken together, the RIM1 S413A-KI mice performed normally in these behavioral tests, and they did not display any of the severe deficits in emotional and spatial learning and memory that were observed in the RIM1α KO mice (27).

Discussion

RIM1α is an active zone protein that is essential for presynaptic short- and long-term plasticity (11, 16, 26). Experiments with cultured cerebellar neurons suggested that phosphorylation of serine-413 of RIM1α by PKA acts as a phospho-switch that controls synaptic strength in a use-dependent manner by modulating the presynaptic release machinery (19). To determine whether a similar mechanism occurs *in vivo* during long-term synaptic plasticity, we set out to test whether phosphorylation of

RIM1α at serine-413 is required for presynaptic long-term plasticity and learning and memory. To achieve this goal, we first searched for specific binding proteins that interact with serine-413 in a phospho-specific manner and then used KI mice to test whether phosphorylation of serine-413 is essential for presynaptic long-term plasticity or learning and memory. In brief, our results demonstrate that although serine-413-phosphorylated RIM1α indeed binds specifically to 14-3-3 proteins, phosphorylation of serine-413 and binding of 14-3-3 proteins are not essential for presynaptic plasticity or for learning and memory.

We found that multiple isoforms of 14-3-3 bind *in vitro* to RIM1α when serine-413 is phosphorylated by PKA but that there are no other tight 14-3-3 binding sites in RIM1α (Fig. 1). We then generated KI mice in which serine-413 is substituted for alanine and phosphorylation at serine-413 is abolished (Fig. 2). We observed that homozygous KI mice are viable and fertile and exhibit no obvious deficits in brain composition, survival, and body weight (Fig. 3). Acute slice recordings revealed that multiple forms of presynaptic long-term and short-term plasticity are normal in the KI mice (Figs. 4 and 5). The KI mice also performed normally in a panel of behavioral tasks (Fig. 6) that are severely impaired in RIM1α KO mice (27). Taken together, we confirm by a targeted genetic mutation that the phosphorylation of RIM1α at serine-413 is not essential for presynaptic long-term plasticity or learning. Because the S413A mutation completely abolished 14-3-3 binding *in vitro*, our data suggest that 14-3-3 binding to RIM1α is also not required for presynaptic long-term plasticity.

Our data raise three questions. First, what experimental differences between this and previous studies might account for the fact that such different conclusions were reached? Second, is it possible that unspecified compensations in the genetic manipulations, as opposed to the rescue experiments using the cultured cerebellar neurons, might have led to the lack of a phenotype? Third, what phosphorylation sites in the presynaptic terminal could alternatively be involved in PKA-dependent presynaptic plasticity given that RIM1α phosphorylation is clearly not essential?

With regard to the experimental differences, it is important to note that previous studies used LTP measurements in cultured neurons in synapses that developed *in vitro* (7, 19). Here, we used acute brain slices for characterizing three distinct and well-defined synapses that exhibit presynaptic long-term plasticity. In all 3 synapses, the S413A mutation in RIM1α did not impair plasticity. The functional properties of synapses in cultures are likely to be different from synapses in acute slices. Moreover, previous studies delivered RIM1α by transfection, driven by a CMV promoter, which might have led to overexpression and/or partial mistargeting of RIM1α or other proteins. In contrast, in the mouse line that we generated, S413A mutant RIM1α was expressed as a KI mutation from the RIM1α promoter at levels that were similar to those of wild-type RIM1α. If RIM1α had been mistargeted, we should have observed a deficit similar to that of RIM1α KO mice. Because long- and short-term plasticity were normal in our experiments, mutant RIM1α was correctly incorporated into the release machinery. Finally, the LTP measurements in cultured cerebellar neurons were performed in constitutive RIM1α KO neurons that developed in the absence of RIM1α, which was only reconstituted a few days before the recordings. In strong contrast, our experiments were performed on neurons that contained all functional domains of RIM1 except for the serine-413 phosphorylation site throughout development.

Although compensation is often invoked when unexpected KO phenotypes are encountered, two observations suggest that compensation cannot explain the lack of a plasticity phenotype in the S413A-KI mice. First, compensation would likely have to occur through RIM2α because RIM2α is the only other RIM isoform that binds to Rab3A. However, the RIM2α deletion on top of the S413A KI did not change the lack of a phenotype in RIM1 S413A-KI mice. Second, if the constitutive mutation of serine-413 in RIM1α did elicit compensation, it would be difficult to understand why the constitutive RIM1α KO would not elicit the same compensation but still exhibited a major plasticity phenotype.

What other phosphorylation sites could act as PKA-triggered phospho-switches during presynaptic LTP? The serine-413 phosphorylation site of RIM1α is conserved in RIM2α, RIM1β (a novel RIM1 isoform; P.S.K. and T.C.S., unpublished observation), and RIM2β, but only the α-isoforms also bind Rab3, which is required for mossy fiber LTP in addition to RIM1α. RIM2α KO mice have no major defects in hippocampal synaptic transmission (25), and our experiments in the RIM1 S413A-KI/RIM2α KO mice show that RIM2α does not compensate for the loss of phosphoserine-413 in RIM1α. We also formally excluded the involvement of RIM1β because in the mutant RIM1 S413A-KI mice, RIM1β also lacks this PKA site (P.S.K and T.C.S., unpublished observation). On the basis of the biochemical data, it seems unlikely that RIM2β participates in presynaptic LTP because it does not bind to Rab3, and RIM2β expression levels are generally low in the dentate gyrus. Furthermore, RIM2β did not compensate for the loss of LTP in RIM1α KO mice (19). RIM1α has an additional PKA phosphorylation site at serine-1548, but according to *in vitro* data it is unlikely that this site participates in LTP because mutant RIM1α that lacked this serine residue still rescued *in vitro* LTP (19). Besides, and in contrast to serine-413, serine-1548 phosphorylation is not prominent in mossy fiber terminals (19). Overall, it is thus unlikely that RIM1α or RIM2α are direct targets of PKA in triggering presynaptic LTP. This conclusion is also in line with the observation that forskolin-dependent potentiation is not abolished in RIM1α KO mice, in which forskolin acts as an activator of adenylyl cyclase and raises the level of total cAMP (16).

Our findings suggest that there are PKA targets other than RIM1α in the presynaptic terminal participating in long-term plasticity. Synapsins have an N-terminal PKA phosphorylation site that regulates binding to synaptic vesicles (28), but synapsins are also not involved in presynaptic LTP (17). Similarly, rabphilin, a Rab3 binding protein (29), is phosphorylated by PKA, but presynaptic LTP is not affected in rabphilin-deficient mice (18). Interestingly, synaptotagmin-12 is a presynaptic PKA target that scales spontaneous release in response to activation of the cAMP-PKA pathway *in vitro* (30). Whether it might play a role in presynaptic long-term plasticity or whether other unknown presynaptic PKA targets are involved remains to be elucidated.

Materials and Methods

Plasmid Construction, Preparation of GST-Fusion Proteins, and Affinity Chromatography. All expression plasmids were constructed in pGEX-KG and purified according to standard methods (31), plasmids were previously reported (19, 32, 33) except pGEX-RIM1 351–429 and 351–596, which were made by PCR from a full-length pCMV-RIM1α expression vector. A detailed methodological description of affinity chromatography can be found in the *SI Text*. In brief, GST-fusion proteins were phosphorylated *in vitro* for 3 h at room temperature and coupled to an Amino-link matrix according the instructions provided with the column (Pierce). Fresh rat brain extracts were incubated with the affinity column overnight at 4°C in the presence of phosphatase inhibitors. Upon multiple elutions at increasing salt concentrations, proteins were visualized with Coomassie and silver staining. The phospho-specific binding partner was identified by mass spectrometry. GST-pulldown assays were performed from native brain homogenates as described (31), and *in vitro* phosphorylation was downscaled accordingly. Brain homogenates were prepared as described in the *SI Text*.

Generation of RIM1 S413A-KI Mice. Mice were generated according to standard procedures (34, 35) and as described in the *SI Text*. By targeting exon 6 of the

RIM1 gene we replaced the serine-413 residue with alanine and introduced BglI and SphI restriction sites for genotyping. The mouse line was submitted to the Jackson Laboratories and is freely available to the community.

Electrophysiology. Synaptic transmission at parallel fiber to Purkinje cell synapses, mossy fiber to CA3 pyramidal cell synapses, inhibitory synapses on CA1 pyramidal cells, and at excitatory Schaffer collateral to CA1 pyramidal cell synapses were recorded in acute slice preparations of 3–6-week old RIM1 S413A mice and littermate control mice according to methods that were previously described (11, 16, 26). Detailed methods and numeric values for each experiment can be found in the *SI Text*. Measurements of mossy fiber LTP were performed in parallel in the laboratories of P.E.C and of R.C.M, and the experimenters were blind to the results of the other laboratory. All other electrophysiological recordings were performed in the laboratory of P.E.C.

Behavior. All behavioral experiments were carried out on RIM1 S413A-KI mice and littermate male wild-type controls at age 3–6 months ($n = 12$ pairs; age difference among pairs <5 weeks). Experimenters were blinded to the genotype and to all electrophysiological analyses during behavioral testing. The order of tests was designed to examine less-stressful behaviors first, with more stressful procedures at the end, and was as follows: locomotor, dark/light box, open field, elevated plus maze, accelerating Rotorod, cue and contextual fear conditioning, and Morris water maze. Mice were moved within the animal facility to the testing room and allowed to habituate to the new location for >1 h before testing. All behaviors were performed as previously described (27). A detailed methodological description can be found in the *SI Text*.

Miscellaneous. SDS/PAGE gels and immunoblotting were performed according to standard methods (34). Most antibodies were previously described (19, 32) or are commercially available (14-3-3ε from Transduction Laboratories, 14-3-3ζ from Santa Cruz Laboratories). The Munc13 antibody was a generous gift from Dr. N. Brose. All data are shown as mean $\pm$ SEM. Statistical significance was determined by the χ^2 test (mouse survival), two-way ANOVA (electrophysiological recordings), or the Student's t test (two-tailed distribution, paired, all other data) where no specific test is stated. All animal experiments were conducted according to the institutional guidelines. Mouse weight studies were performed on male littermate pairs, and the mice were weighed every 2 days from postnatal day 6 through 14 and then on postnatal days 18, 24, and 60.

ACKNOWLEDGMENTS. We thank E. Borowicz, J. Mitchell, I. Kornblum, and L. Fan for excellent technical assistance; Dr. Robert Hammer for blastocyst injections of embryonic stem cells; and members of the Sudhof laboratory for comments and advice. This work was supported by grants from the National Institutes of Health (P01 NS053862 from the National Institute of Neurological Disorders and Stroke to T.C.S. and R.C.M., DA17392 to P.E.C., MH065975 to C.M.P.), by a Swiss National Science Foundation Postdoctoral Fellowship (to P.S.K.), a Hirschl/Weill-Caulier Career Scientist Award (to P.E.C.), by the Blue Gator Foundation (to C.M.P.), and National Alliance for Research on Schizophrenia and Depression Young Investigator Awards (to P.S.K. and C.M.P.).

1. Kandel ER (2001) The molecular biology of memory storage: A dialogue between genes and synapses. *Science* 294:1030–1038.
2. Nicoll RA, Malenka RC (1999) Expression mechanisms underlying NMDA receptor-dependent long-term potentiation. *Ann N Y Acad Sci* 868:515–525.
3. Hansel C, Linden DJ, D'Angelo E (2001) Beyond parallel fiber LTD: The diversity of synaptic and non-synaptic plasticity in the cerebellum. *Nat Neurosci* 4:467–475.
4. Nicoll RA, Malenka RC (1995) Contrasting properties of two forms of long-term potentiation in the hippocampus. *Nature* 377:115–118.
5. Nicoll RA, Schmitz D (2005) Synaptic plasticity at hippocampal mossy fibre synapses. *Nat Rev Neurosci* 6:863–876.
6. Salin PA, Malenka RC, Nicoll RA (1996) Cyclic AMP mediates a presynaptic form of LTP at cerebellar parallel fiber synapses. *Neuron* 16:797–803.
7. Linden DJ, Ahn S (1999) Activation of presynaptic cAMP-dependent protein kinase is required for induction of cerebellar long-term potentiation. *J Neurosci* 19:10221–10227.
8. Spencer JP, Murphy KP (2002) Activation of cyclic AMP-dependent protein kinase is required for long-term enhancement at corticostriatal synapses in rats. *Neurosci Lett* 329:217–221.
9. Castro-Alamancos MA, Calcagnotto ME (1999) Presynaptic long-term potentiation in corticothalamic synapses. *J Neurosci* 19:9090–9097.
10. Chevaleyre V, Castillo PE (2003) Heterosynaptic LTD of hippocampal GABAergic synapses: A novel role of endocannabinoids in regulating excitability. *Neuron* 38:461–472.
11. Chevaleyre V, Heifets BD, Kaeser PS, Sudhof TC, Castillo PE (2007) Endocannabinoid-mediated long-term plasticity requires cAMP/PKA signaling and RIM1alpha. *Neuron* 54:801–812.
12. Hirano T (1991) Differential pre- and postsynaptic mechanisms for synaptic potentiation and depression between a granule cell and a Purkinje cell in rat cerebellar culture. *Synapse* 7:321–323.
13. Xiang Z, Greenwood AC, Kairiss EW, Brown TH (1994) Quantal mechanism of long-term potentiation in hippocampal mossy-fiber synapses. *J Neurophysiol* 71:2552–2556.
14. Nguyen PV, Woo NH (2003) Regulation of hippocampal synaptic plasticity by cyclic AMP-dependent protein kinases. *Prog Neurobiol* 71:401–437.
15. Castillo PE, *et al.* (1997) Rab3A is essential for mossy fibre long-term potentiation in the hippocampus. *Nature* 388:590–593.
16. Castillo PE, Schoch S, Schmitz F, Sudhof TC, Malenka RC (2002) RIM1alpha is required for presynaptic long-term potentiation. *Nature* 415:327–330.
17. Spillane DM, Rosahl TW, Sudhof TC, Malenka RC (1995) Long-term potentiation in mice lacking synapsins. *Neuropharmacology* 34:1573–1579.
18. Schluter OM, *et al.* (1999) Rabphilin knock-out mice reveal that rabphilin is not required for rab3 function in regulating neurotransmitter release. *J Neurosci* 19:5834–5846.
19. Lonart G, *et al.* (2003) Phosphorylation of RIM1alpha by PKA triggers presynaptic long-term potentiation at cerebellar parallel fiber synapses. *Cell* 115:49–60.
20. Simsek-Duran F, Linden DJ, Lonart G (2004) Adapter protein 14-3-3 is required for a presynaptic form of LTP in the cerebellum. *Nat Neurosci* 7:1296–1298.
21. Leger J, Kempf M, Lee G, Brandt R (1997) Conversion of serine to aspartate imitates phosphorylation-induced changes in the structure and function of microtubule-associated protein tau. *J Biol Chem* 272:8441–8446.
22. Ku NO, Liao J, Omary MB (1998) Phosphorylation of human keratin 18 serine 33 regulates binding to 14-3-3 proteins. *EMBO J* 17:1892–1906.
23. Bridges D, Moorhead GB (2004) 14-3-3 proteins: A number of functions for a numbered protein. *Sci STKE* 2004:re10.
24. Sun L, Bittner MA, Holz RW (2003) Rim, a component of the presynaptic active zone and modulator of exocytosis, binds 14-3-3 through its N terminus. *J Biol Chem* 278:38301–38309.
25. Schoch S, *et al.* (2006) Redundant functions of RIM1alpha and RIM2alpha in Ca(2+)-triggered neurotransmitter release. *EMBO J* 25:5852–5863.
26. Schoch S, *et al.* (2002) RIM1alpha forms a protein scaffold for regulating neurotransmitter release at the active zone. *Nature* 415:321–326.
27. Powell CM, *et al.* (2004) The presynaptic active zone protein RIM1alpha is critical for normal learning and memory. *Neuron* 42:143–153.
28. Hosaka M, Hammer RE, Sudhof TC (1999) A phospho-switch controls the dynamic association of synapsins with synaptic vesicles. *Neuron* 24:377–387.
29. Ostermeier C, Brunger AT (1999) Structural basis of Rab effector specificity: Crystal structure of the small G protein Rab3A complexed with the effector domain of rabphilin-3A. *Cell* 96:363–374.
30. Maximov A, Shin OH, Liu X, Sudhof TC (2007) Synaptotagmin-12, a synaptic vesicle phosphoprotein that modulates spontaneous neurotransmitter release. *J Cell Biol* 176:113–124.
31. Okamoto M, Sudhof TC (1997) Mints, Munc18-interacting proteins in synaptic vesicle exocytosis. *J Biol Chem* 272:31459–31464.
32. Wang Y, Okamoto M, Schmitz F, Hofmann K, Sudhof TC (1997) Rim is a putative Rab3 effector in regulating synaptic-vesicle fusion. *Nature* 388:593–598.
33. Wang Y, Liu X, Biederer T, Sudhof TC (2002) A family of RIM-binding proteins regulated by alternative splicing: Implications for the genesis of synaptic active zones. *Proc Natl Acad Sci USA* 99:14464–14469.
34. Ho A, *et al.* (2006) Genetic analysis of Mint/X11 proteins: Essential presynaptic functions of a neuronal adaptor protein family. *J Neurosci* 26:13089–13101.
35. Rosahl TW, *et al.* (1993) Short-term synaptic plasticity is altered in mice lacking synapsin I. *Cell* 75:661–670.